

RESEARCH ARTICLE

Open Access



Molecular damage and responses of oral keratinocyte to hydrogen peroxide

Kuan-Yu Lin¹, Ching-Hung Chung², Jheng-Sian Ciou³, Pei-Fang Su⁴, Pei-Wen Wang⁵, Dar-Bin Shieh^{2,5,6*} and Tzu-Chueh Wang^{7*}

Abstract

Background: Hydrogen peroxide (H₂O₂)-based tooth bleaching reagents have recently increased in popularity and controversy. H₂O₂ gel (3%) is used in a Nightguard for vital bleaching; transient tooth sensitivity and oral mucosa irritation have been reported. Genotoxicity and carcinogenicity have also been significant concerns.

Methods: We used primary cultured normal human oral keratinocytes (NHOKs) as an in vitro model to investigate the pathological effects to mitochondria functions on human oral keratinocytes exposed to different doses of H₂O₂ for different durations.

Results: An MTT assay showed compromised cell viability at a dose over 5 mM. The treatments induced nuclear DNA damage, measured using a single-cell gel electrophoresis assay. A real-time quantitative polymerase chain reaction showed H₂O₂ induced significant increase in mitochondrial 4977-bp deletion. Mitochondrial membrane potential and apoptosis assays suggested that oxidative damage defense mechanisms were activated after prolonged exposure to H₂O₂. Reduced intracellular glutathione was an effective defense against oxidative damage from 5 mM of H₂O₂.

Conclusion: Our study suggests the importance for keratinocyte damage of the dose and the duration of the exposure to H₂O₂ in at-home-bleaching. A treatment dose ≥ 100 mM directly causes severe cytotoxicity with as little as 15 min of exposure.

Keywords: Tooth bleaching, Molecular genetics, Oxidative stress, Toxicology, Keratinocyte(s)

Background

Tooth color contributes significantly to a person's aesthetic appearance. Normal tooth color is determined by the optical and chromatic properties of dentine and enamel: hue, value, chroma, thickness, texture, and translucency [1]. Both intrinsic and extrinsic factors in dentin or enamel, or in both, can cause tooth discoloration [1–3]. Nightguard vital bleaching (at-home-bleaching) was first introduced in 1989 to reduce tooth discolorations [4]. The 10% carbamide peroxide used in a custom-fitted nightguard was converted by saliva in the oral cavity to 3% H₂O₂ (~ 0.9 M) and 7% urea [3–5]. H₂O₂ diffuses into the enamel-dentine junction and dentine, and using a redox reaction, decomposes chromogens, which whitens teeth

[2, 6]. The most noteworthy side effects associated with at-home-bleaching are tooth sensitivity and oral mucosa irritation. Some studies [5, 7, 8], however, report that these side effects are transient and can be recovered from after treatment. Safety for exposure to a long-term H₂O₂ bleaching agent has also been a concern in more recent studies [9, 10]. H₂O₂ generates free radicals, especially hydroxyl radical, in oxidative reactions; free radicals are considered genotoxic and carcinogenic [11, 12]. Long-term exposure to high-dose H₂O₂ can damage soft and hard oral tissue [4, 6]. The inappropriate application or abuse of H₂O₂ during cleaning treatments has other potential adverse effects [13].

We explored the pathological effects of H₂O₂ on gingival mucosa under different concentration doses and exposure durations using primary cultured normal human oral keratinocytes (NHOKs) as a model. Gingival mucosa is composed of highly-regenerative keratinized stratified squamous epithelium and submucosal connective tissues.

* Correspondence: dbshieh@mail.ncku.edu.tw; tzchwa@mail.cnu.edu.tw

²Department of Stomatology, National Cheng-Kung University Hospital, Tainan 70101, Taiwan

⁷Department of Pharmacy, Chia-Nan University of Pharmacy and Science, Tainan 71710, Taiwan

Full list of author information is available at the end of the article



The NHOKs in the epithelium form a barrier to defend basal cells with regenerative capability from chemical and physical insults of oral environment including the reactive oxygen species generated during tooth bleaching [14]. Through previous oral transmucosal bioavailability studies, various factors were known to reduce the chemical exposure to basal cells thus reducing the actual H₂O₂ concentration at this level from tooth bleaching [15]. The keratinized gingival mucosa is known to harbor a lower permeability, intermediate residence time, and high blood flow as compared to the buccal and palatal mucosa [16, 17]. H₂O₂ gel also effectively reduced risk of high dose exposure to oral mucosa compared to the liquid form [18]. Besides, the EU Commission established in the cosmetics directive that the concentration of hydrogen peroxide in consumer oral hygiene products should be limited to 0.1% [19]. Therefore, we tested the proposed equivalent exposure dose at basal level in the range of 0.01~100 mM (0.000033% ~ 0.33%) in this study. The mechanism of H₂O₂-induced cell death was further explored by assessing mitochondrial membrane potential- and apoptosis-related pathways. The antioxidant defense system was also investigated for its role in the short- and the long-term exposure.

Methods

Normal human Oral keratinocytes: Primary cultures

Gingival tissue was isolated from excess tissue during the surgical removal of impacted wisdom teeth from 10 healthy patients (age 19~50) under approval by NCKUH Institutional Review Board for Human Studies. The specimens were incubated in 1 mL of Keratinocyte-SFM medium (KGM; Gibco BRL, Gaithersburg, MD, USA) containing dispase (5 mg/mL) (Gibco) at 4 °C for overnight. The epithelial tissue was separated from the specimens and washed with phosphate-buffered saline (PBS) containing penicillin, streptomycin, and fungizone (PSF 100X; Gibco) before the specimens were dissected into smaller pieces (about 1 mm³). The tube was centrifuged at 800 rpm for 5 min, and then the pellet was transferred to another tube containing 1 mL of 0.25% trypsin (Gibco) and incubated at 37 °C for 5–7 min. One milliliter of 0.25% trypsin inhibitor (Gibco) and KGM (1 mL) were subsequently added. The tube was centrifuged again at 1200 rpm for 5 min and the pellet was resuspended with KGM (5 mL) and then incubated in a T25 flask containing 100X lincomycin (10 mg/mL) (Sigma-Aldrich, St. Louis, MO, USA). The procedure was modified from Kim et al. [20], and the cells were plated with a density < 80% for the initiation of treatment. The pooled NHOKs samples from 10 donors were used within 3rd to 10th passages. The NHOKs were characterized periodically for microscopic presentation and their intermediate filament expression profile (keratin+, vimentin-) as well as free of mycoplasma contamination by qPCR. The results well defined the

NHOKs in this study. The pooled NHOKs were used for all tests and the experiments were triplicated.

Comet assay

NHOKs (2 × 10⁵/well) were seeded in 6-well plates overnight and then the old medium was replaced with new medium containing different doses of H₂O₂ for 1 h or 8 h. Comet assays (single cell gel electrophoresis [SCGE]) were performed according to the manufacturer's instructions (Trevigen, Gaithersburg, MD, USA). Briefly, 10 μL of the resuspended solution was mixed with melted 75 μL of 1.5% LM agarose then 50 μL of the final mixture was immediately placed onto a CometSlide™. The slides were then placed at 4 °C in the dark for 15 min before immersed in 4 °C lysis solution for 1 h. The slides were then immersed in alkaline DNA unwinding solution (pH > 13.0) at 25 °C in the dark for 30 min and placed in an electrophoresis tray. Electrophoresis was performed (30 Volt 300 mA) for 20 min and the slides were then processed in neutralization buffer for 5 min for 3 times, then immersed in methanol for 5 min. The slides were dried at 37 °C for another 5 min then stained by 100 μL of diluted SYBR Green I (Ex = 450–490 nm; Em = 510 nm) for 30 min. After electrophoresis, levels of DNA damage were quantified by the presence of “comet tail” viewed under epifluorescence microscopy, where the migration of DNA toward the anode increased as the frequency of single strand break (SSB) increased. One hundred cells were randomly selected from each slide to calculate the DNA damage level with comet assay software. The damage levels were determined by tail moment (TM) and calculated by the following equations.

$$\text{Tail length}(TL, \%) = (\text{content extent} - \text{head extent}) / \text{comet extent} \times 100\%$$

$$\text{Tail intensity}(TI, \%) = (\text{comet integrated intensity} - \text{head intensity}) / \text{comet integrated intensity} \times 100\%$$

$$\text{Tail moment}(TM) = TL \times TI$$

Total DNA isolation

NHOKs (5 × 10⁵/well) were seeded with different doses of H₂O₂ and incubated for 1 h or 8 h. The cells were then harvested and counted after they had been stained with 0.4% trypan blue dye (Sigma-Aldrich). They were then transferred to 1.5-mL microtubes, and DNA was isolated using Trizol (Sigma-Aldrich). The final precipitated DNA was dissolved in 100 μL of ddH₂O and calculated for the concentration by spectrophotometer (2000c, NanoDrop, Wilmington, DE, USA) at 260/280 nm.

mtDNA⁴⁹⁷⁷ deletion assay

The mitochondrial DNA copy number and the ratio of mtDNA⁴⁹⁷⁷ deletion to the total mtDNA were determined using a real-time quantitative polymerase chain reaction

(qPCR) and Power Sybr Green (Applied Biosystems, Foster City, CA, USA) in a qPCR system (StepOne™; Applied Biosystems) as previously described [21]. The primers designed for quantification of total mtDNA were listed as follow: L11 5′-ATACAGACCAAGAGCCT-3′ (forward; nt5527–5543) and H11 5′-GCGGGAGAAGTAGATTGA-3′ (reverse; nt5722–5739). The mtDNA⁴⁹⁷⁷ deletion was determined by targeting the template spanning from nt8469 to nt13447 with the primers: L1 5′-AACCAACACCTCTTTACAGTGAA-3′ (forward; nt8342–8364) and H1 5′-GATGATGTGGTCTTTGGAGTAGAA-3′ (reverse; nt13501–13524). Δ mtDNA⁴⁹⁷⁷ deletion data obtained from qPCR were calculated with the following equation. Δ mtDNA⁴⁹⁷⁷ deletion = mtDNA⁴⁹⁷⁷/total mtDNA.

Quantitating reduced glutathione

NHOKs (2×10^5 /well) were treated with different doses of H₂O₂ for 1 h or 8 h and then harvested. The cells were incubated at 37 °C for 20 min with 500 μ L of 1X 20- μ M of CellTracker Green CMFDA Dye (Molecular Probes, Eugene, OR, USA) and then centrifuged at 1200 rpm (241 g) for another 5 min. They were then washed three times with 500 μ L of PBS, resuspended, and transferred to flow tubes. The glutathione (GSH) content, determined using CMFDA (green, Ex = 522 nm; Em = 595 nm), was quantitated using a flow cytometer (FACSCalibur; BD Biosciences, Franklin Lakes, NJ, USA) at the FL1-H channel, as previously described [22].

Apoptosis assay

H₂O₂-treated NHOKs (1×10^6 /mL) were harvested and resuspended in annexin-V binding buffer (BioVision, Milpitas, CA, USA). A 100- μ L aliquot of the solution was transferred to a 5-mL culture tube, and 5 μ L of annexin V-FITC (BD Biosciences) was added. The cells were gently mixed and then incubated for 15 min at room temperature in the dark. At the end of the inoculation period, 400 μ L of annexin V binding buffer was added to each flow tube. Late and early apoptosis was evaluated using the flow cytometer and analyzed using WinMDI 2.9 software (The Scripps Research Institute; <http://www.cyto.purdue.edu/flowcyt/software/Winmdi.htm>) [23].

Cell viability assay

An MTT (1-(4,5-dimethylthiazol-2-yl)-3,5-diphenylformazan) assay was used to measure cell viability, as previously described [24]. Briefly, the MTT reagents were added to the cultured cells subject to different concentrations and exposure period of H₂O₂ with a final concentration at 0.5 mg/mL. The cells were then incubated for 3 h at 37 °C. The medium was removed and DMSO was added into each well to dissolve the formazan.

Finally, the cell viability was determined by the optical absorption at 490 nm referenced to the control.

Mitochondrial membrane potential ($\Delta\Psi_m$) analysis

JC-1 (5,5′,6,6′-tetrachloro-1,1′,3,3′-tetraethylbenzimidazolcarbocyanine iodide) (Molecular Probes) was used to quantify $\Delta\Psi_m$ (monomers at a low $\Delta\Psi_m$ presented a green fluorescent emission [green, Ex = 488 nm; Em = 527 nm] and aggregates formed at a high $\Delta\Psi_m$ showed red fluorescence [red, Ex = 488 nm; Em = 590 nm]). NHOKs (2×10^5 cells/well) were seeded in 6-well plates and incubated overnight before treated with different concentrations of H₂O₂ for either 1 h or 8 h. The test media were removed, then the cells were harvested and washed with PBS before adding 500 μ L of 10 μ M JC-1 was added to the media followed by gentle vortex. The cells were incubated at 37 °C for 20 min, then centrifuged at 1200 rpm (241 g) for 5 min, and then the pellet was washed 3 times in 500 μ L of PBS. The cells were re-suspended in 500 μ L of PBS and then transferred to a flow tube for FACS analysis (FACS-Calibur; BD Biosciences, Franklin Lakes, NJ, USA). The ratio between red and green JC-1 fluorescence signals was calculated from data acquired in the flow cytometer at FL1-H and FL2-H, as previously described [24].

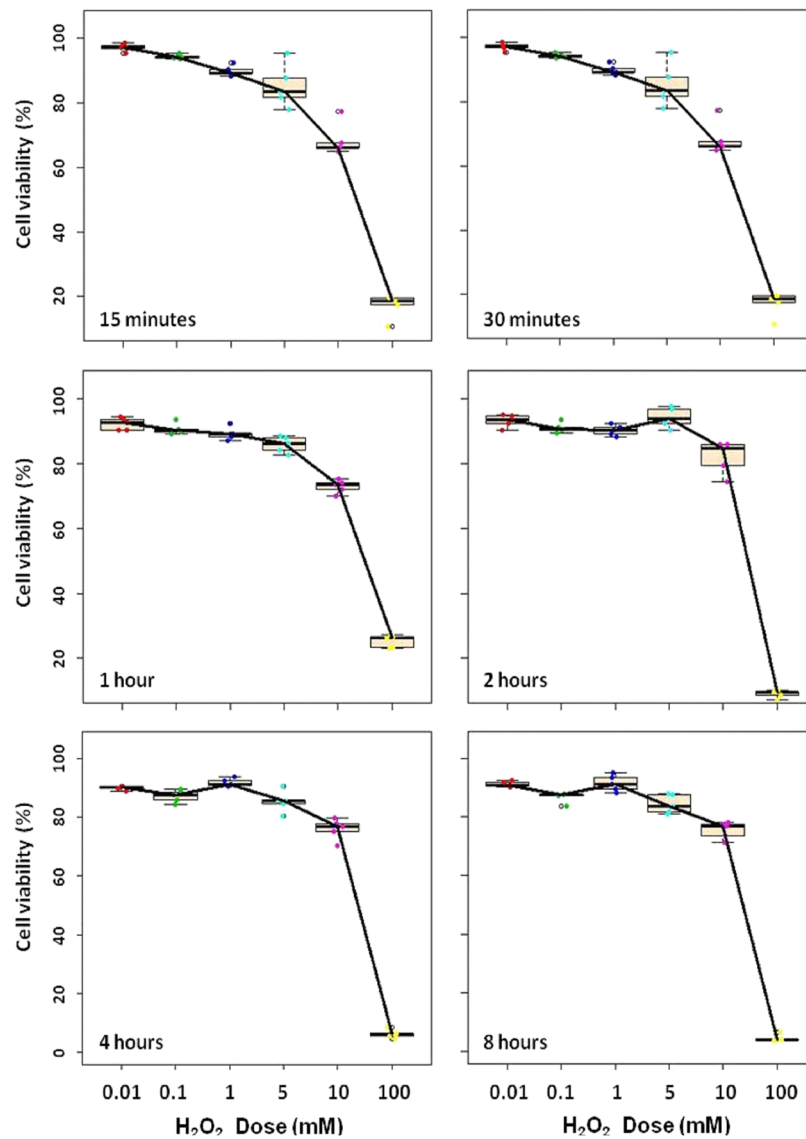
Results

Nuclear DNA damage and cell cytotoxicity were higher in cells treated with H₂O₂

Cell viability based on the dose of H₂O₂ was analyzed by MTT assay, which showed that regardless of the incubation period (between 15 min and 8 h); the H₂O₂-treated NHOKs were > 90% viable when treated with 0.01–1 mM of H₂O₂. After the NHOKs had been treated with 5 mM of H₂O₂, however, their viability was significantly lower: about 85%. Moreover, cell viability was inversely dependent upon exposure time and dose: the longer and higher they respectively were, the lower was cell viability. Cells treated with > 5 mM of H₂O₂ were significantly less viable (Fig. 1). The critical dose for a significant and substantial reduction in cell viability for all exposure times was 5 mM (Fig. 1a). A more detailed dosage analysis (1–10 mM in 1-mM increments) showed that viability was dose-dependent as well as time-dependent (Fig. 1b). We chose 5 mM of H₂O₂ as the treatment dose.

An alkaline comet assay was used to observe the nuclear DNA (nDNA) damage caused by H₂O₂-induced oxidative attacks. The tail moment (the product of the tail length and the fraction of total DNA in the tail) was significantly H₂O₂-dependent (Fig. 2a). The tail moment increased substantially but nonsignificantly: it doubled (and was otherwise dose-dependent except at 100 mM) after the NHOKs had been exposed to 5 mM of H₂O₂ for 1 h.

A.



B.

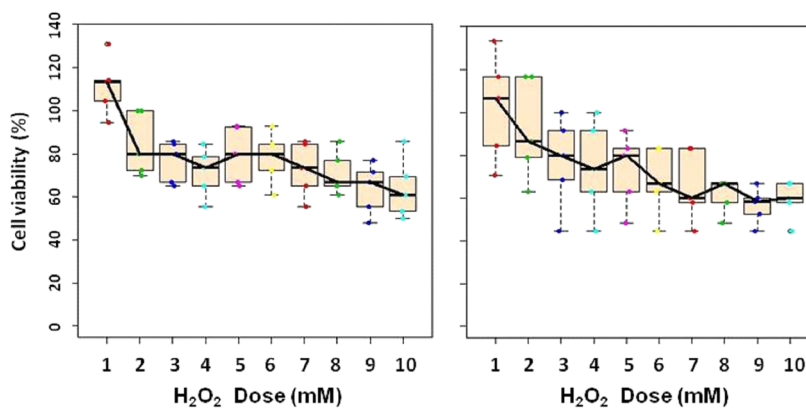
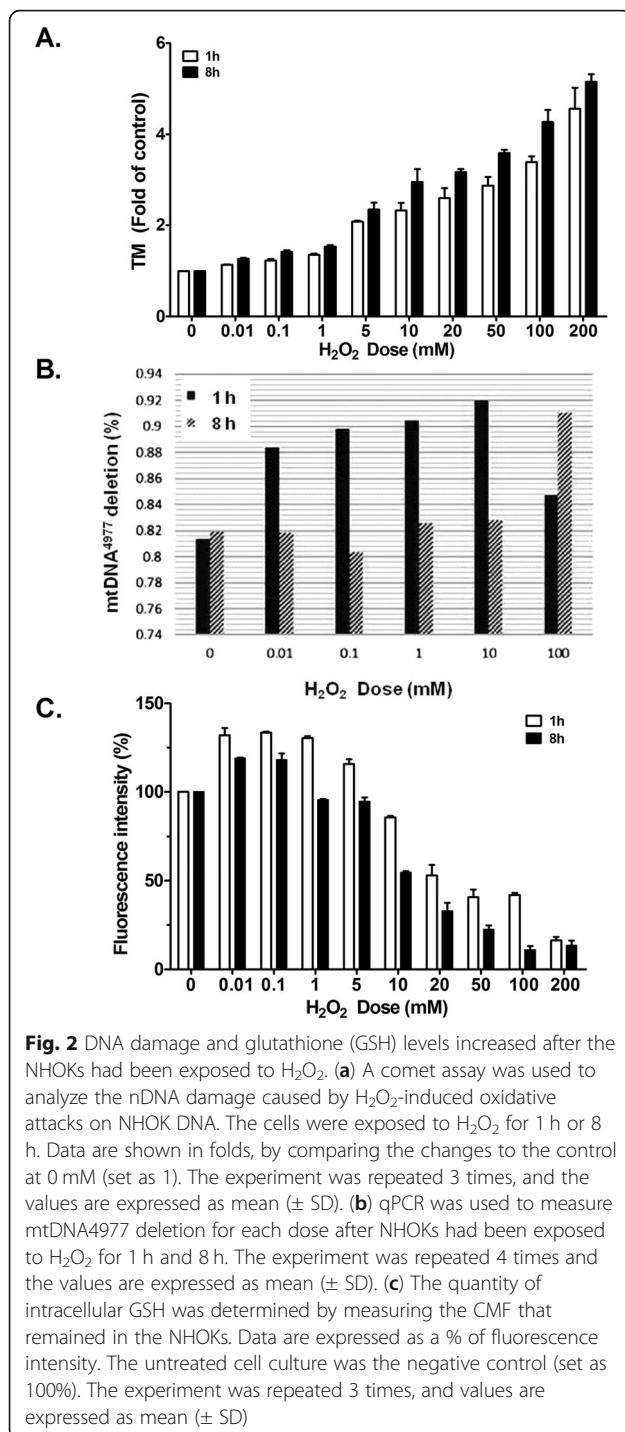


Fig. 1 Cell viability of NHOKs after they had been exposed to different doses of H₂O₂ for different durations. **(a)** NHOKs were seeded in medium containing H₂O₂ (range: 0.01–100 mM). The cells were incubated for 15 min, 30 min, 1 h, 2 h, 4 h, and 8 h. Cell viability in culture medium alone was the negative control. The experiment was repeated 5 times. **(b)** Cell viability of NHOKs cultured in medium containing 10 different doses of H₂O₂ (range: 1–10 mM). The experiment was repeated 5 times



Mitochondrial DNA (mtDNA) deletion and glutathione inhibition increased after the NHOKs had been briefly exposed to H₂O₂

The *in vitro* mtDNA⁴⁹⁷⁷ deletion assay showed that NHOKs contained an average of 0.81% of the baseline ratio. After 1 h of treatment with 0.01–10 mM of H₂O₂, mtDNA⁴⁹⁷⁷ deletion was dose-dependently higher, but after treatment with 10 mM of H₂O₂, mtDNA⁴⁹⁷⁷

deletion was back at 85% of the baseline level. However, mtDNA⁴⁹⁷⁷ deletion did not significantly change in NHOKs treated with a dose of H₂O₂ < 10 mM for 8 h. Only after the NHOKs had been treated with 100 mM H₂O₂ for 8 h did mtDNA⁴⁹⁷⁷ deletion significantly increase to 0.91% (Fig. 2b).

The glutathione (GSH): oxidized glutathione (GSSG) ratio was inversely related to the proportion of mtDNA⁴⁹⁷⁷ deletion. GSH levels were significantly higher after NHOKs had been exposed to H₂O₂ (0.01 and 5 mM) for 1 h. However, GSH was significantly and dose-dependently lower after they had been exposed to doses > 10 mM. In 8 h of treatment, excess GSH was generated after treatment with 0.01 and 0.1 mM of H₂O₂, but when treatment doses were > 1 mM, GSH levels were lower (Fig. 2c). Not only was there a dose-dependent effect, but GSH levels were also time-dependently lower at all doses.

The effect of H₂O₂ treatment on NHOK apoptosis activation via the loss of mitochondrial membrane potential

Flow cytometric analysis showed NHOKs undergoing apoptosis in the annexin-V FITC-positive/PI (pyridium iodide)-negative population, and undergoing necrosis in the annexin-V FITC-negative/PI-positive population. After the NHOKs had been exposed to H₂O₂ for 1 h, there was a dose-dependent increase in the level of apoptotic cells, which began to fall when the dose was > 100 mM. In the 8-h treatment group, at doses < 10 mM, apoptosis was dose-dependently higher, but it gradually decreased when doses were > 20 mM (Fig. 3a, b).

We also analyzed the cellular apoptosis pathway with JC-1 staining as a marker for mitochondrial membrane potential ($\Delta\Psi_m$). The loss of $\Delta\Psi_m$ is an early event in intrinsic mitochondrial-mediated apoptosis. The FL1:FL2 fluorescence ratio reflects the status of $\Delta\Psi_m$: a higher value indicates that more $\Delta\Psi_m$ has been lost. Within 1 h, the $\Delta\Psi_m$ levels returned to normal when H₂O₂ doses were < 1 mM. A significant amount of $\Delta\Psi_m$ was lost, which was indicated by the 407-fold rise in the fluorescence ratio (Fig. 3c) when the treatment dose was \geq 5 mM. However, the lost $\Delta\Psi_m$ was partially restored at 8 h to 27-fold that of the controls. An increase in lost $\Delta\Psi_m$ was significant at 8 h when treatment doses were between 0.01 and 5 mM, which was about 10-fold that of the negative.

Discussion

After we exposed NHOKs to H₂O₂, we comprehensively evaluated the effects on cell viability, DNA damage, cellular defense response to oxidative damage, and apoptosis in the estimated basal cell level exposure dose range of 0.01~100 mM, which is about 1/10 that of the H₂O₂ in the bleaching gel. From the dose- and duration-dependent decrease in cell viability, we confirmed that exposing

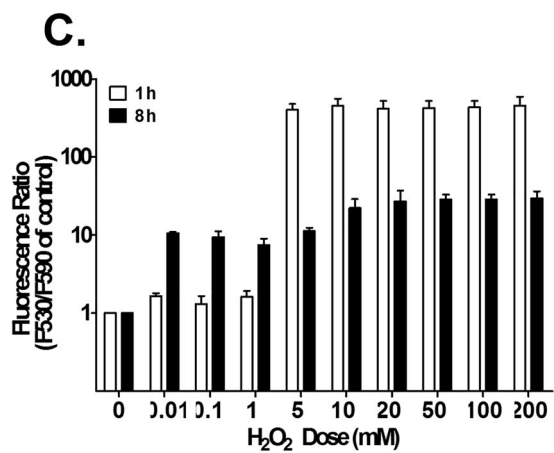
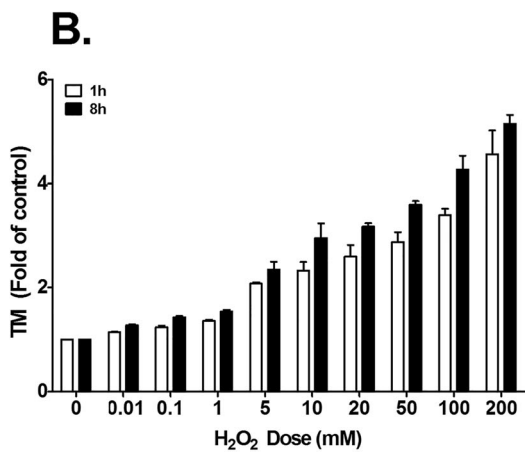
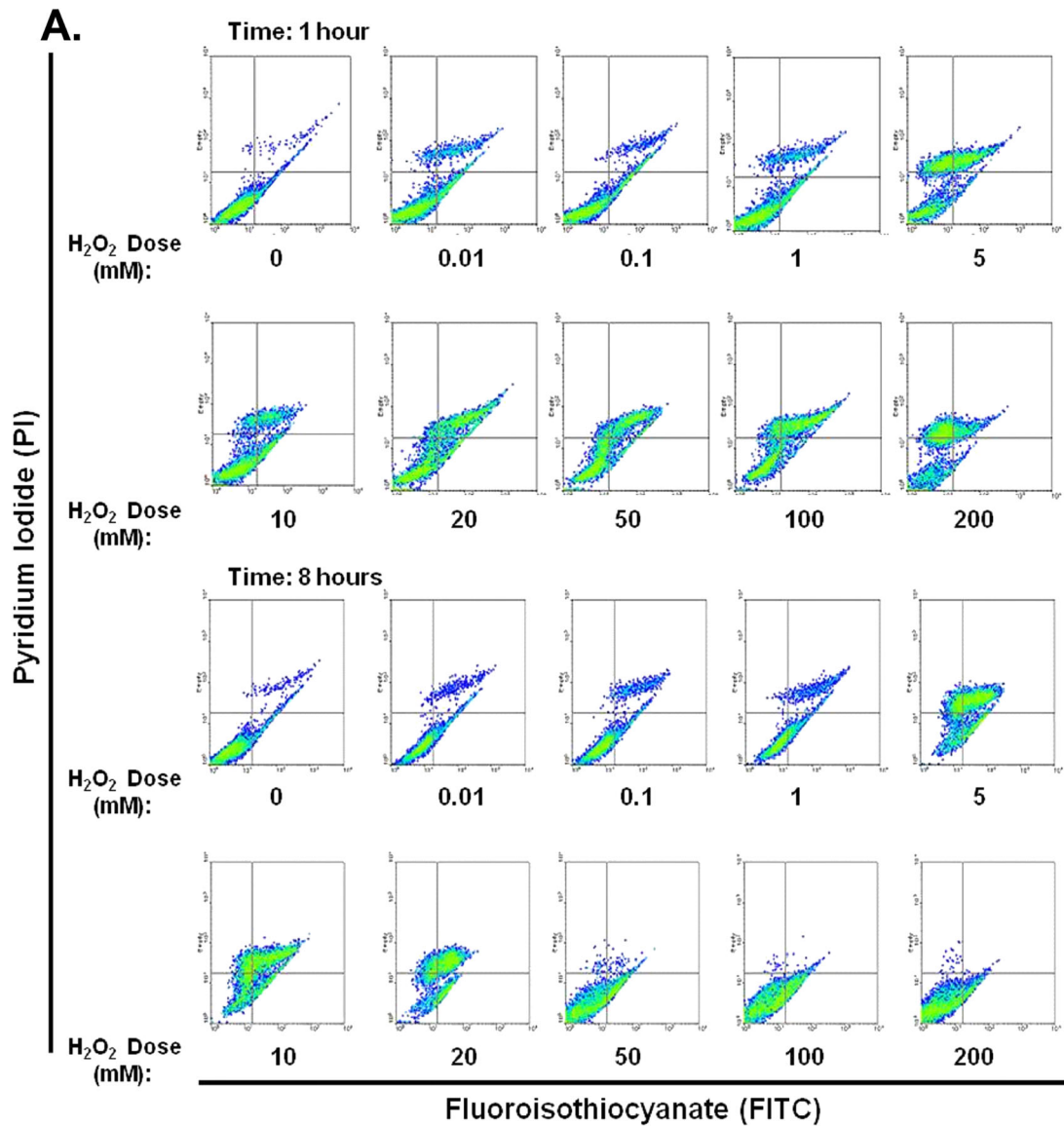


Fig. 3 (See legend on next page.)

(See figure on previous page.)

Fig. 3 NHOK apoptosis activation by H₂O₂ treatment through mitochondrial membrane potential ($\Delta\Psi_m$) loss. **(a)** Annexin V-FITC/PI for 1 h and 8 h. **(b)** % apoptosis was calculated from the results in Fig. 3A. The Controls showed normal levels of apoptosis. The experiment was repeated 3 times, and the values are expressed as mean (\pm SD). **(c)** JC-1 was used to measure $\Delta\Psi_m$ by comparing the amounts of green (F530) and orange fluorescence (F590). The fluorescence ratios (F530/F590) were then compared with that of the Controls (set as 1) and expressed in folds, to provide a clear view of the $\Delta\Psi_m$ after exposing the NHOKs to H₂O₂ for either 1 h or 8 h. The experiment was repeated 3 times, and the values are expressed as mean (\pm SD)

NHOKs to H₂O₂ induced significant cellular damage, especially when the dose exceeded 5 mM. The study also revealed that the degree of cell proliferation inhibition was dose- and duration-dependent. This finding is consistent with O'Toole et al., who used a similar dose range: 2, 4, and 7 mM [25]. They reported that a low dose of H₂O₂ have no effect on NHOKs viability at doses $\leq 700 \mu\text{M}$ for even after exposure for 24 h. We found that $>90\%$ cell survival could be maintained using doses $< 1 \text{ mM}$, even after 8 h of exposure, which is the exposure time to Night-guard vital bleaching.

Dental bleaching is based on the ability of H₂O₂ to penetrate through tooth structure and produce free radicals to oxidize the colored organic molecules. There are many reports investigated the effect of dose and exposure time of H₂O₂ to the pulpal tissues as the bleaching agents penetrated through the tooth structure [26–28]. However, only few addressed the effect of acute or chronic exposure of the leaked bleaching agents to oral mucosal keratinocytes. Although 3% H₂O₂ was most commonly used for tooth bleaching, the actual exposure dose of to the basal cell layer of oral mucosa that regenerate the mucosal barrier was affected by multiple factors. At one end, the peroxide releases into saliva from home bleaching systems require to diffuse through the carrier while being diluted and degraded by the saliva. It has been reported that gel formulation significantly reduced the peroxide concentration in the saliva more than that of the liquid form [27]. The leaked peroxide was rapidly degraded by the saliva to 52 and 24% of the original concentrations at 2 and 6 h after exposure, respectively [29]. The remaining salivary H₂O₂ needs to penetrate deep into the basal layer and subgingival tissues through epithelium barrier to exert pathological effects [30]. According to EU recommend oral hygiene products, the tissue exposure of H₂O₂ concentration should be limited to 0.1% or 29.4 mM. In this study, the direct exposure at dose range of 0.01 mM to 100 mM was applied using primary cultured gingival oral keratinocyte as the model. The pathological effects of both short (1 h) and long (8 h) exposures were analyzed according to the common clinical practices.

The safety of H₂O₂ tooth bleaching is still controversial: its genotoxicity and carcinogenicity are under active discussion [9, 10]. Diaz-Llera et al. showed that 0.34–1.35 μM of H₂O₂ induced hypoxanthine guanine phosphoribosyltransferase (HPRT) mutation both in vitro

and in vivo [31]. High-dose H₂O₂ was reported to be mildly carcinogenic for the duodenum of catalase-deficient mice [9]. In another report, 1% H₂O₂ ($\sim 0.3 \text{ M}$) in drinking water induced forestomach tumors in rats [10]. These reports showed that exposure to high-dose H₂O₂ for a sustained period induces oxidative stress that leads to DNA damage in mammalian cells.

In this study, we used primary cultured NHOKs isolated from the basal layer of oral gingival epithelium that is closely related to the most susceptible cell types in clinical practice of tooth bleaching (gingival mucosa). The primary cultured NHOKs presented similar properties of basal layer keratinocytes that maintained certain replication and differentiation potential suitable for study the peroxide induced DNA damage and subsequent pathogenic signaling. Unlike nDNA, mtDNA lacks histone protections and sophisticated DNA repair mechanisms to shelter it from oxidative attacks [32, 33]. Free radical attacks normally cause mtDNA mutation, deletion, or other types of damage and can be preserved in the cells in heteroplasmic format. One common type of mtDNA damage is the 4977-bp deletion (*nt8469–13,447*) that is related to aging [34, 35] and to different diseases, such as Kearns-Sayre syndrome [36]. A comet assay confirmed that H₂O₂ induced nDNA damage. In the tested dose range of 0.01 to 200 mM, we found that the number of nDNA single strand breaks was dose-dependent. Interestingly, only the difference in nDNA damage between 1 and 8 h of exposure to each dose of H₂O₂ was significant. However, we found no plateau dose in the treatment range.

The comet assay showed only nDNA damage but not mtDNA damage [37]. We thus used qPCR to quantify the ratio of mtDNA damage. For the control NHOKs, mtDNA⁴⁹⁷⁷ deletion showed only 0.81% baseline deletion in vitro. During the first hour of exposure to H₂O₂, mtDNA⁴⁹⁷⁷ deletion dose-dependently increased. Despite a significant drop in the mtDNA deletion ratio at a dose of 100 mM H₂O₂, we suspect that it can be attributed to direct massive cellular damage, which was supported by the MTT assay. After the NHOKs had been exposed to H₂O₂ for 8 h, all groups but the 100-mM treatment group were restored to their approximate baseline levels. This confirmed that H₂O₂ can be genotoxic to both nDNA and mtDNA in NHOKs. Moreover, in keratinocytes treated with $< 10 \text{ mM}$ of H₂O₂ for 8 h,

mtDNA⁴⁹⁷⁷ deletion, but not nDNA, returned to normal. This is consistent with Ballinger et al., who used two treatment doses (0.1 and 0.5 mM) for 1 h [32].

Croteau and Bohr [38] reported that mitochondria are more efficient at DNA repair than nDNA, and that mitochondria are able to repair 65% of the lesions within 4 h. However, nDNA has a more sophisticated defense and repair mechanism than does mtDNA because it includes histone protection and nucleotide excision repair. Both nDNA and mtDNA damage contribute to carcinogenesis [39]. Therefore, the genotoxicity of both mtDNA and nDNA should be a concern for people who use at-home-bleaching over the long term.

Unlike nDNA damage, mtDNA damage can be preserved in a heteroplasmic state, thus allowing cells to survive and proliferate when the damage is repairable [40]. Both normal and damaged mtDNA copies can be amplified and passage in the organelles. A large-scale deletion would affect the supply of essential proteins in the electron transport chain, thus interfering with the normal function of mitochondria; this can be considered a loss of $\Delta\Psi_m$ [41]. In the present study, $\Delta\Psi_m$ was low at 8 h, as well as it was after 1 h, which was consistent with the treatment-time-associated alterations in the ratio of mtDNA⁴⁹⁷⁷ deletion. A dramatic (~ 407-fold) increase in $\Delta\Psi_m$ loss occurred within 1 h after NHOKs had been treated with doses < 1 mM. For longer exposure (8 h), the degree of $\Delta\Psi_m$ loss was attenuated to between 10- and 30-fold, and it occurred with doses as low as 0.01 mM. Thus, mtDNA⁴⁹⁷⁷ deletion seemed to be more sensitive to oxidative attacks than was $\Delta\Psi_m$ to the dose and duration of exposure to H₂O₂, which is conceivable because replacing a protein complex in damaged DNA takes time through transcription and translation. The same reason applied for the observation that after 8 h, $\Delta\Psi_m$ loss occurred even at doses as low as 0.01 mM, while the ratio of mtDNA⁴⁹⁷⁷ deletion had already been restored at doses < 100 mM.

Oxidative attacks induce various types of cell death: apoptosis, autophagy, and necrosis [42–44]. These cell death mechanisms are in fact not completely disadvantageous: they prevent severely damaged cells from contributing to the development of cancer. After 1 h of exposure to H₂O₂, the number of apoptotic cells dose-dependently increased, and the apoptotic fraction dropped significantly at doses > 200 mM. The number of necrotic cells increased at doses > 5 mM. At the highest dose (200 mM), a large number of NHOKs became necrotic instead of apoptotic, as evidenced by a large PI-positive population. After 8 h of exposure, apoptosis was also dose-dependent, but the apoptotic cell population rapidly fell when treatment doses were > 50 mM. The necrotic population grew as the apoptotic population declined.

At lower levels of oxidative attack, pro-apoptotic Bcl-2 family proteins increase mitochondrial membrane permeability and stimulate voltage-dependent anion

channel (VDAC) activity which reduces H⁺ and $\Delta\Psi_m$ in the inner membrane, as shown in our $\Delta\Psi_m$ assay. When the matrix expands to rupture the outer membrane, cytochrome *c* and apoptosis-inducing factor are released to the cytoplasm to induce cell apoptosis [45–47]. The observed timing and dose response in our experiments support this model. In addition, a drastic decline of cell viability at high doses of H₂O₂ should be a primary consequence of direct chemically induced necrosis, but apoptosis was activated at low doses of H₂O₂.

In addition to DNA repair and various types of cell death, activation of antioxidant molecular mechanisms is important for cellular defense against at-home-bleaching-induced health hazards. It is known that catalase and GSH are essential for the cellular antioxidant defense system, and that they detoxify H₂O₂-induced damage in vivo [48]. GSH is one of the most important nonenzymatic antioxidants that exist in large amounts within cells, including in mitochondria [22]. Thus, measuring GSH content in response to different doses of H₂O₂ should provide important mechanistic insights. After the first hour of treatment, GSH levels were higher than at baseline when H₂O₂ doses were between 0.01 mM and 5 mM. This was followed by a dose-dependent decline from 86 to 16% of baseline in the dose range of 10 mM to 200 mM, which implies that at lower doses, a protective increase in GSH was activated. At a high dose, however, the endogenous GSH was rapidly consumed to protect cells against oxidative attacks. After the NHOKs had been exposed to H₂O₂ for 8 h, excess GSH was detected when the dose was < 0.1 mM, but the levels were significantly lower than they had been. At higher doses, dose-dependent decreases in GSH were detected, but they were consistently lower than they had been at the same doses. These findings implied that a negative balance between GSH generation and consumption occurred during continuous exposure to H₂O₂.

Conclusion

Our study showed the importance for keratinocyte damage affected by the dose and the duration of H₂O₂ exposure in at-home-bleaching. A treatment dose ≥ 100 mM directly causes severe cytotoxicity within as little as 15 min of exposure. According to other reports [49], saliva can readily convert high doses (~ 1.6 M) of H₂O₂ to as little as 0.029 mM in 20 min. At such doses, mtDNA⁴⁹⁷⁷ deletion is expected to slightly increase and the apoptotic population to double during the first hour of exposure. The deletion ratio will be restored after 8 h of exposure, but apoptotic cells will quadruple in number. However, GSH at such a high treatment dose was significantly elevated and fewer nDNA breaks were detected. To verify the biological safety and feasibility of H₂O₂ tooth bleaching for long-term use, additional in vivo studies in which the local tissue environment and circulation factors are controlled must be conducted.

Abbreviations

GSH: glutathione; GSSG: oxidized glutathione; H₂O₂: Hydrogen peroxide; HPRT: hypoxanthine guanine phosphoribosyltransferase; JC-1: 5, 5', 6, 6'-tetrachloro-1, 1', 3, 3'-tetraethylbenzimidazolcarboyanine iodide; KGM: Keratinocyte-SFM medium; mtDNA: mitochondrial DNA; MTT: 1-(4, 5-dimethylthiazol-2-yl)-3, 5-diphenylformazan; nDNA: nuclear DNA; NHOKs: normal human oral keratinocytes; PBS: phosphate-buffered saline; PI: pyridium iodide; PSF: penicillin streptomycin and fungizone; qPCR: real-time quantitative polymerase chain reaction; SCGE: single cell gel electrophoresis; SSB: single strand break; TI: Tail intensity; TL: Tail length; TM: tail moment; VDAC: voltage-dependent anion channel; $\Delta\Psi_m$: mitochondrial Membrane Potential

Acknowledgements

We thank Mr. Li-Xing Yang and Miss Li-Fang Chiu for their technical support. This work was supported by the Center of Applied Nanomedicine, National Cheng Kung University from The Featured Areas Research Center Program within the framework of the Higher Education Sprout Project by the Ministry of Education (MOE) in Taiwan.

Funding

This work was funded by the Ministry of Science and Technology of Taiwan (MOST 104-2314-B-006-063-MY3 and MOST 105-2627-M-006-001-). The authors declare that the funding body played no role in the design of the study, the collection, analysis, and interpretation of the data and in writing the manuscript.

Availability of data and materials

All data generated or analyzed during this study are included in this published article. The RAW data supporting this study can be obtained by contacting the corresponding authors.

Authors' contributions

KY Lin prepared the draft of this manuscript and performed the experiments. CH Chung provided clinical insight and draft part of the manuscript. JS Ciou finalized the detail study protocols and complete the experiments with KY Lin. PF Su helped the data analysis and statistics. PW Wang integrated opinions from the authors to revise the manuscript and helped the response to the reviewers. DB Shieh and TC Wang initiate the whole study idea and made a series of revisions of this manuscript. They also mentor the research progress and finalized the manuscript submission. All authors have read and approved the final manuscript.

Ethics approval and consent to participate

The research protocol and consent form were approved by the Institutional Review Board (IRB) for Human Studies of National Cheng Kung University Medical Center (approval ID: A-BR-102-017). Informed consents from all patients who donated samples were collected. All patients aware their samples may be used for this scientific research. The samples were taken as part of routine care during surgical extraction of wisdom teeth.

Consent for publication

Not applicable.

Competing interests

The authors declare that they have no competing interests.

Publisher's Note

Springer Nature remains neutral with regard to jurisdictional claims in published maps and institutional affiliations.

Author details

¹Department of Biochemistry and Molecular Biology, Pennsylvania State University, State College, Harrisburg, PA 16803, USA. ²Department of Stomatology, National Cheng-Kung University Hospital, Tainan 70101, Taiwan. ³Graduate Institute of Pharmaceutical Science, Chia-Nan University of Pharmacy and Science, Tainan 71710, Taiwan. ⁴Department of Statistics, National Cheng Kung University, Tainan 70101, Taiwan. ⁵Institute of Oral Medicine and Department of Stomatology, College of Medicine, National Cheng Kung University Hospital, National Cheng Kung University, Tainan 70101, Taiwan. ⁶Center of Applied Nanomedicine, Center for Micro/Nano Science and Technology, Advanced Optronic Technology Center, Innovation Center for Advanced Medical Device Technology, National Cheng Kung University, Tainan 70101, Taiwan. ⁷Department of Pharmacy, Chia-Nan University of Pharmacy and Science, Tainan 71710, Taiwan.

Received: 8 March 2017 Accepted: 17 December 2018

Published online: 11 January 2019

References

- Suliman MA. An overview of tooth-bleaching techniques: chemistry, safety and efficacy. *Periodontol* 2000. 2008;48:148–69.
- Joiner A, Thakker G, Cooper Y. Evaluation of a 6% hydrogen peroxide tooth whitening gel on enamel and dentine microhardness in vitro. *J Dent*. 2004; 32(Suppl 1):27–34.
- Plotino G, Buono L, Grande NM, et al. Nonvital tooth bleaching: a review of the literature and clinical procedures. *J Endodontics J Endod*. 2008;34(4): 394–407.
- Haywood VB, Heymann HO. Nightguard vital bleaching. *Quintessence Int*. 1989;20(3):173–6.
- Li Y. Biological properties of peroxide-containing tooth whiteners. *Food Chem Toxicol*. 1996;34(9):887–904.
- Buchalla W, Attin T. External bleaching therapy with activation by heat, light or laser—a systematic review. *Dent Mater*. 2007;23(5):586–96.
- dos Santos Medeiros MC, de Lima KC. Effectiveness of nightguard vital bleaching with 10% carbamide peroxide—a clinical study. *J Can Dent Assoc*. 2008;74(2):163.
- Haywood VB, Heymann HO. Nightguard vital bleaching: how safe is it? *Quintessence Int*. 1991;22(7):515–23.
- Munro IC, Williams GM, Heymann HO, et al. Tooth whitening products and the risk of oral cancer. *Food Chem Toxicol*. 2006;44(3):301–15.
- Naik S, Tredwin CJ, Scully C. Hydrogen peroxide tooth-whitening (bleaching): review of safety in relation to possible carcinogenesis. *Oral Oncol*. 2006;42(7):668–74.
- Cadet J, Douki T, Gasparutto D, et al. Oxidative damage to DNA: formation, measurement and biochemical features. *Mutat Res*. 2003;531(1–2):5–23.
- Williams GM, Jeffrey AM. Oxidative DNA damage: endogenous and chemically induced. *Regul Toxicol Pharmacol*. 2000;32(3):283–92.
- Li Y, Greenwall L. Safety issues of tooth whitening using peroxide-based materials. *Br Dent J*. 2013;215(1):29–34.
- Calenic B, Greabu M, Caruntu C, Tanase C, Battino M. Oral keratinocyte stem/progenitor cells: specific markers, molecular signaling pathways and potential uses. *Periodontol* 2000. 2015 Oct;69(1):68–82. <https://doi.org/10.1111/prd.12097>.
- Alqahtani MQ. Tooth-bleaching procedures and their controversial effects: A literature review. *Saudi dent J*. 2014;26(2):33–46. <https://doi.org/10.1016/j.sdentj.2014.02.002>.
- de Vries ME, Boddé HE, Verhoef JC, Junginger HE. Developments in buccal drug delivery. *Crit Rev Ther Drug Carrier Syst*. 1991;8(3):271–303.
- Squier CA, Nanny D. Measurement of blood flow in the oral mucosa and skin of the rhesus monkey using radiolabelled microspheres. *Arch Oral Biol*. 1985;30(4):313–8.
- Marson FC, Gonçalves RS, Silva CO, Cintra LT, Pascotto RC, Santos PH, Briso AL. Penetration of hydrogen peroxide and degradation rate of different bleaching products. *Oper Dent*. 2015 Jan-Feb;40(1):72–9. <https://doi.org/10.2341/13-270-L>. Epub 2014 May 14.
- EU (European Union). Risk assessment report, hydrogen peroxide. 2003 Vol 38, EU, Brussels.
- Kim MS, Li SL, Bertolami CN, et al. State of p53, Rb and DCC tumor suppressor genes in human oral cancer cell lines. *Anticancer Res*. 1993; 13(5A):1405–13.
- Shieh DB, Chou WP, Wei YH, et al. Mitochondrial DNA 4,977-bp deletion in paired oral cancer and precancerous lesions revealed by laser microdissection and real-time quantitative PCR. *Ann N Y Acad Sci*. 2004; 1011:154–67.
- Tarpey MM, Wink DA, Grisham MB. Methods for detection of reactive metabolites of oxygen and nitrogen: in vitro and in vivo considerations. *Am J Physiol Regul Integr Comp Physiol*. 2004;286(3):R431–44.
- Abedini MR, Wang PW, Huang YF, et al. Cell fate regulation by gelsolin in human gynecologic cancers. *Proc Natl Acad Sci U S A*. 2014;111(40):14442–7.
- Wang PW, Abedini MR, Yang LX, et al. Gelsolin regulates cisplatin sensitivity in human head-and-neck cancer. *Int J Cancer*. 2014;135(12):2760–9.
- O'Toole EA, Goel M, Woodley DT. Hydrogen peroxide inhibits human keratinocyte migration. *Dermatol Surg*. 1996;22(6):525–9.
- Torres CR, Souza CS, Borges AB, Huhtala MF, Caneppele TM. Influence of concentration and activation on hydrogen peroxide diffusion through

- dental tissues in vitro. *Sci World J.* 2013 Sep 18;2013:193241. <https://doi.org/10.1155/2013/193241> eCollection 2013.
27. Hannig C, Zech R, Henze E, Dreier S, Attin T. Peroxide release into saliva from five different home bleaching systems in vivo. *Am J Dent.* 2005 Feb; 18(1):13–8.
 28. Hanks CT, Fat JC, Wataha JC, Corcoran JF. Cytotoxicity and dentin permeability of carbamide peroxide and hydrogen peroxide vital bleaching materials, in vitro. *J Dent Res.* 1993;72(5):931–8.
 29. Matis BA. Degradation of gel in tray whitening. *Compend Contin Educ Dent Suppl.* 2000;(28):S28, S31–5; quiz S49.
 30. Tipton DA, Braxton SD, Dabbous MK. Role of saliva and salivary components as modulators of bleaching agent toxicity to human gingival fibroblasts in vitro. *J Periodontol.* 1995 Sep;66(9):766–74.
 31. Diaz-Llera S, Podlutzky A, Osterholm AM, et al. Hydrogen peroxide induced mutations at the HPRT locus in primary human T-lymphocytes. *Mutat Res.* 2000;469(1):51–61.
 32. Ballinger SW, Patterson C, Yan CN, et al. Hydrogen peroxide- and peroxyxynitrite-induced mitochondrial DNA damage and dysfunction in vascular endothelial and smooth muscle cells. *Circ Res.* 2000;86(9):960–6.
 33. Clayton DA. Transcription of the mammalian mitochondrial genome. *Annu Rev Biochem.* 1984;53:573–94.
 34. Lee HC, Pang CY, Hsu HS, et al. Ageing-associated tandem duplications in the D-loop of mitochondrial DNA of human muscle. *FEBS Lett.* 1994;354(1): 79–83.
 35. Linnane AW, Baumer A, Maxwell RJ, et al. Mitochondrial gene mutation: the ageing process and degenerative diseases. *Biochem Int.* 1990;22(6):1067–76.
 36. Zeviani M, Moraes CT, DiMauro S, et al. Deletions of mitochondrial DNA in Kearns-Sayre syndrome. *Neurology.* 1988;38(8):1339–46.
 37. Hartmann A, Agurell E, Beevers C, et al. Recommendations for conducting the in vivo alkaline comet assay. 4th international comet assay workshop. *Mutagenesis.* 2003;18(1):45–51.
 38. Croteau DL, Bohr VA. Repair of oxidative damage to nuclear and mitochondrial DNA in mammalian cells. *J Biol Chem.* 1997;272(41):25409–12.
 39. Tokarz P, Blasiak J. Role of mitochondria in carcinogenesis. *Acta Biochim Pol.* 2014;61(4):671–8.
 40. McFarland R, Chinnery PF, Blakely EL, et al. Homoplasmy, heteroplasmy, and mitochondrial dystonia. *Neurology.* 2007;69(9):911–6.
 41. Chatterjee A, Mambo E, Sidransky D. Mitochondrial DNA mutations in human cancer. *Oncogene.* 2006;25(34):4663–74.
 42. Baker K, Staecker H. Low dose oxidative stress induces mitochondrial damage in hair cells. *Anat Rec (Hoboken).* 2012;295(11):1868–76.
 43. Bouchier-Hayes L, Lartigue L, Newmeyer DD. Mitochondria: pharmacological manipulation of cell death. *J Clin Invest.* 2005;115(10):2640–7.
 44. Valko M, Leibfritz D, Moncol J, et al. Free radicals and antioxidants in normal physiological functions and human disease. *Int J Biochem Cell Biol.* 2007; 39(1):44–84.
 45. Orrenius S. Reactive oxygen species in mitochondria-mediated cell death. *Drug metabolism reviews Drug Metab Rev.* 2007;39(2–3):443–55.
 46. Shimizu S, Konishi A, Kodama T, et al. BH4 domain of antiapoptotic Bcl-2 family members closes voltage-dependent anion channel and inhibits apoptotic mitochondrial changes and cell death. *Proc Natl Acad Sci U S A.* 2000;97(7):3100–5.
 47. Tsujimoto Y, Shimizu S. VDAC regulation by the Bcl-2 family of proteins. *Cell Death Differ.* 2000;7(12):1174–81.
 48. Bergendi L, Benes L, Duracková Z, et al. Chemistry, physiology and pathology of free radicals. *Life Sci.* 1999;65(18–19):1865–74.
 49. Mahony C, Barker ML, Engel TM et al. Peroxide degradation kinetics of a direct application percarbonate bleaching film. *Am J Dent.* 2003; 16(Spec No):9B-11B.

Ready to submit your research? Choose BMC and benefit from:

- fast, convenient online submission
- thorough peer review by experienced researchers in your field
- rapid publication on acceptance
- support for research data, including large and complex data types
- gold Open Access which fosters wider collaboration and increased citations
- maximum visibility for your research: over 100M website views per year

At BMC, research is always in progress.

Learn more biomedcentral.com/submissions

